4BCO2 EDU Performance

Warren T Peters[1]
NASA Marshall Space Flight Center, Huntsville, AL, 35812

Gregory E. Cmarik[2]
Jacobs Space Exploration Group, Huntsville, AL, 35812

James C. Knox[3]
Dynetics Technical Services, Huntsville, AL, 35812

NASA is reducing the power, volume and mass requirements on future Carbon Dioxide (CO2) removal systems for exploration missions. To meet this goal, a 4BCO2 flight experiment based on Four Bed Molecular Sieve (4BMS) technology is under construction and will fly to International Space Station (ISS) for on-orbit performance and reliability testing. The 4BCO2 flight experiment was based on the 4BMS-X Engineering Development Unit (EDU) design, which has been modified to incorporate elements of the flight system. This paper will present the operational performance of the 4BCO2 EDU.

Nomenclature

ISS	=	International Space Station	*Linus*	=	Nickname for 4BCO2 EDU
CO2	=	Carbon Dioxide	*dP*	=	Delta Pressure
CDRA	=	Carbon Dioxide Removal Assembly	*Dwp*	=	Dew Point
CDRA4EU	=	CDRA-4 Engineering Unit	*RPM*	=	Rotations Per Minute
NASA	=	National Aeronautics and Space Administration	*ISS*	=	International Space Station
MSFC	=	Marshall Space Flight Center	*RTD*	=	Resistance Temperature Detector
4BMS	=	4-bed molecular sieve	*ppCO2*	=	CO2 Partial Pressure
4BCO2	=	4-Bed Carbon Dioxide Scrubber Flight Demo	*F*	=	Fahrenheit
EDU	=	Engineering Development Unit	*GPM*	=	Gallons per minute
LTL	=	Low Temperature Loop	*RPM*	=	Rotations Per Minute
SCFM	=	Standard (0°C, 1 atm) Cubic Feet per Minute	*hc*	=	Half Cycle Time Duration
DAB	=	Desiccant-Adsorbent Bed	*PID*	=	Proportional Integral Derivative
COTS	=	Commercial off the Shelf			

I. Introduction

This paper communicates the test data generated from the ground 4-bed molecular sieve (4BMS) system used as the basis for the 4-Bed Carbon Dioxide Scrubber Flight Demo (4BCO2) flight experiment. This ground system, named 4BMS-X[1], was developed to improve the performance and reliability of a four-bed CO2 removal system. Changes are described in detail in *4-Bed CO2 Scrubber – From Design to Build*[2], a short summary is included here: reduced adsorbent mass in both desiccant and adsorbent beds, cylindrical bed shapes, cartridge heater and radiator core to suit the cylindrical shape, reduction of Grace 544 13X in the desiccant bed, Grace 544 13X replaced ASRT[3-5] in the adsorbent beds, improved precooler, and replacement air-save pump. While building the flight 4BCO2 heater core, we manufactured a duplicate heater core and installed it into the ground system to make a direct comparison to the flight 4BCO2 system. We nicknamed the ground test Engineering Development Unit (EDU) *Linus* after the cartoon character. *Linus* is not an acronym, it's simple to type and reminds us the purpose of this system is to learn and question, which fits his character. Note, Grace 544 13X will be stated simply as 13X for the remainder of the paper.

[1] Aerospace Engineer, NASA, and MSFC/ES62.
[2] ECLSS Engineer, Jacobs Space Exploration Group, and MSFC/ES62.
[3] Aerospace Engineer, Dynetics Technical Services, and MSFC/ES62.

Hardware configuration

We designed Linus with a flexible structure that allows rapid removal and replacement of various components. The configuration described in this paper is the 5th configuration tested to date. We installed a heritage Honeywell blower in-line with the valves and precooler for a brief test program last year, but it was removed to retain as much life as possible for the upcoming flight program. The facility pushes air to the test article, so we placed a hinged 'vent' just upstream of the test article inlet to decouple the amount the facility pushes versus the amount the test article pulls using the blower. This should closely simulate the ISS configuration where the inlet airline is attached to a large diameter plenum.

Differences Between Linus EDU and Flight 4BCO2 Configuration

1. For this test series, we routed air from Valve 103 to an industrial blower mounted on the floor shown in Fig. 1. The geometric configuration of the air supply does not affect CO2 removal performance metrics, only total flow.
2. In order to simplify facility duct fabrication, 2 weeks total fabrication time, we used Commercial-Off-The-Shelf (COTS) vacuum duct components. The duct layout is slightly different than the flight unit, but produces the same system air dP within 2 in-H2O pressure drop. See Figure 1.
3. All air selector valves are COTS items, except the MSFC-built valve 104 which features a re-pressurization port.
4. The ground system and facility has > 100 sensor, versus 16 sensors installed on the flight system.
5. Controlled by desktop computer and LABView applications, but uses the same control logic and set points.

Identical Features Between Linus EDU and Flight 4BCO2 Configuration

1. Heater core: Linus total heater power for 1 adsorbent bed = 700W within 5 Watts of the flight power.
2. Precooler: same design and manfucaturer, but ~20% less surface area than flight due to additional seal requirements
3. Valve 104 uses the low-dust MSFC design that incorporates the slow re-pressurization feature
4. Adsorbent materials: same layering, but flight beds hold ~2% more due to manufacturing details, Figure 2
5. Adsorbent bed removable filters: flight uses a different O-ring seal configuration, but the element is the same
6. Air-save pump: same Scroll Labs X-50 model, but uses commercial controller and cooling fan

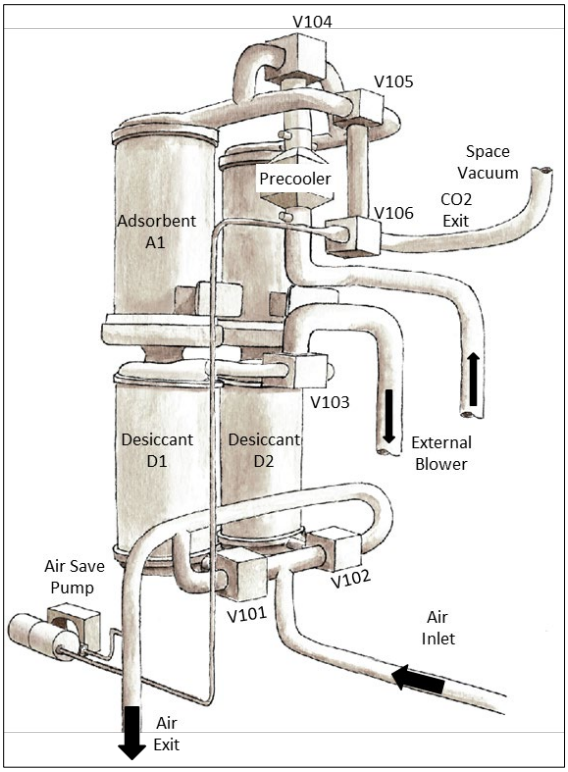

Fig 1. Physical System Configuration

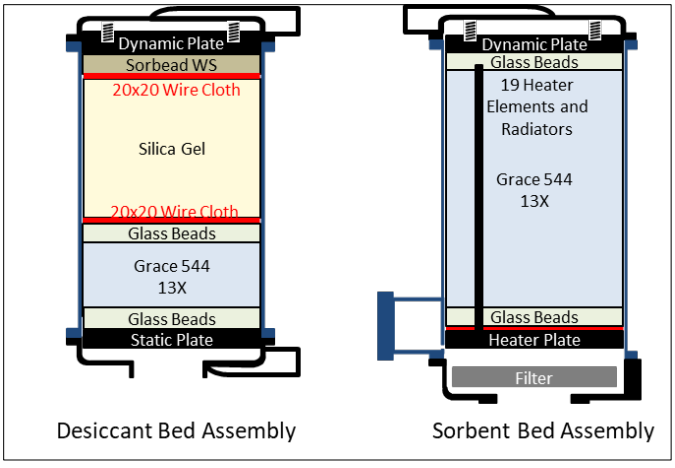

Fig 2. Bed Material Layering

II. Instrumentation and Error Calculations

Additional instrumentation allows us to see the cause-effect relationship within the system, as well as providing the basis for optimizing system performance. To insure accurate performance calculations, we installed duplicate measurements in locations critical to performance, as well as calculating the CO2 mass balance, shown in Figure 3.

1. One flow measurement is used for calculations, and the other used for comparison
2. One CO2 concentration measurement is used for calculations, and the other used for comparison. The inlet CO2 concentration sensor is standardized to calibration gas once per test series (about 4 tests).
3. At the end of a half cycle, this CO2 sensor is equal to the inlet CO2 concentration.
4. CO2 mass is measured by the flow controller and compared to the change in CO2 bottle mass.
5. CO2 mass injected by the flow controller is compared to the amount of CO2 mass required to create the inlet air CO2 concentration at that flowrate. This is the mass balance check.
6. The exit CO2 sensor (used to calculate how much CO2 does not reach the CO2 exit) is compared to a separate sensor as well as standardization using calibration gases.
7. At the end of a half cycle, the adsorbent bed internal RTD's read similar to the precooler outlet air RTD.

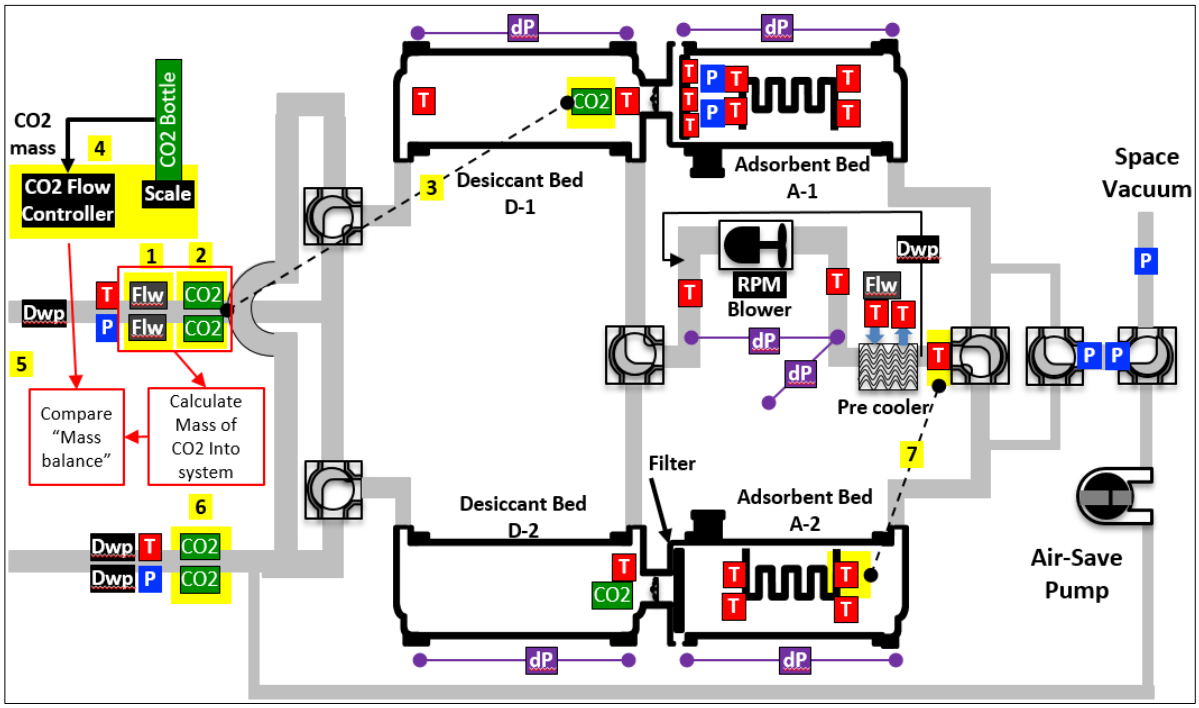

Fig 3. Linus Schematic: P=pressure, T=temperature, Flw=Flow, Dwp=Dew Point, CO2=Concentration, dP=delta Pressure

III. Boundary Conditions

We set boundary conditions for the test series consistent with the ranges we expect to see on ISS. We began testing with an Low Temperature Loop (LTL) temperature of 51F to compare to a previous test series, but switched to 41.5F to match expected conditions for the 4BCO2 payload location. The inlet air dew point and temperature depend on ISS conditioning requirements for a particular location, so we chose a dew point of 49F and a dry bulb temperature of 56F because these fall near the center of the expected range. We used a 120V power supply to run the internal bed heaters because the 4BCO2 payload location supplies 120Vdc power. We iterated the CO2 vacuum system conductance until the maximum pressure during desorption matched that of a similar CDRA-4EU case, which was designed to match the ISS configuration for CDRA.

The program levied a requirement to remove 4.16 kg/day of CO2 using an inlet CO2 partial pressure (ppCO2) of 2 torr. We controlled the ppCO2 to 2 torr as we performed sensitivity testing, however, we also performed limited testing at higher CO2 partial pressure because future missions will likely use a higher ppCO2 value. This has substantial implications for system performance and optimization, which will be explored in future testing.

IV. Time-Varying System Responses

The time-varying parameters displayed in the graphs provide insight for the interaction with ISS systems and the basis for performance variations. Half cycle (hc) listed below is time elapsed for the airsave-adsorb-vacuum modes.

Table 1

Inlet air flow	Inlet Air Temp	Inlet air Dwp	ppCO2	hc	PC H2O temp	PC H2O Flow
26 scfm	56 F	49 F	2 torr	10-60-10	51 F	0.52 gpm

Conditions controlled constant for this test series, dwp = dew point, pc = precooler, temp = temperature.

Only the central 7 heater elements are turned on during air-save mode, with the outer 12 added during the rest of the half cycle. The heater design[6] creates even power/area in the adsorbent volume. The outer 12 heater elements use more power because the outer region of the cylindrical bed has a larger volume. The average bed temperature reaches 400F in 62 minutes, allowing for the possibility of reducing the half cycle time, shown in figure 4. Moisture may condense in the air exit for ~ 2 minutes when the heat wave firsts exits the desiccant bed[6], shown in figure 5.

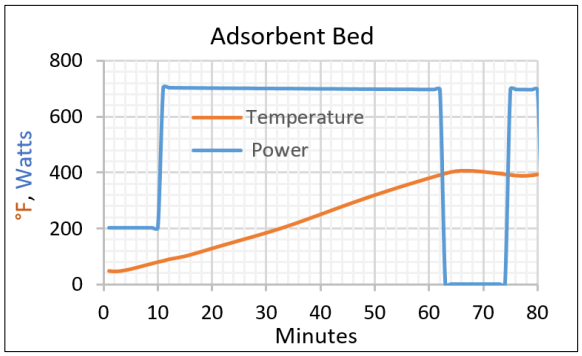

Figure 4. Adsorbent Bed Power and Temperature

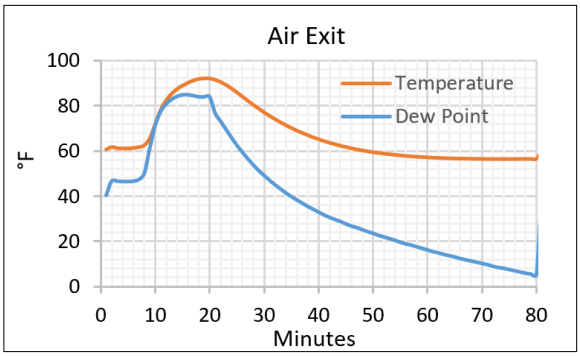

Figure 5. Air Leaving System Exit

CO2 held in the desiccant bed 13X is released from the air exit at the beginning of the half cycle, creating the large initial CO2 spike exiting the system air exit, shown in figure 6. CO2 is held in the desiccant bed 13X and never reaches the adsorbent bed for removal from the system. *CO2 Holdup* accounts for a major part of our efficiency loss. Future work to replace the desiccant bed 13X with a material that does not adsorb CO2 could increase performance. Very little CO2 leaves the air exit at the end of the half cycle, indicating a shorter half cycle would not increase performance because system CO2 breakthrough is small. A higher inlet ppCO2 would accelerate system CO2 breakthrough and a shorter half cycle could increase CO2 removal.

We controlled inlet air volumetric flow to insure the same total mass into the system as we compared test points. Volumetric flow was held constant using a PID controlled loop that varied blower RPM. The flight system will command a constant RPM, and we switched to that control method for the last 3 tests and will use it for the next test series. There was no discernable performance difference if the blower was set to deliver the same half-cycle-averaged flow, shown in figure 7.

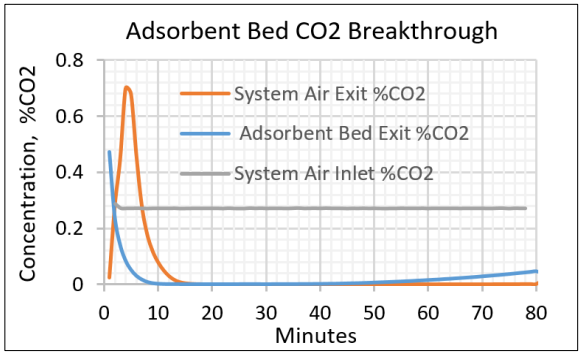

Figure 6. Breakthrough Curves

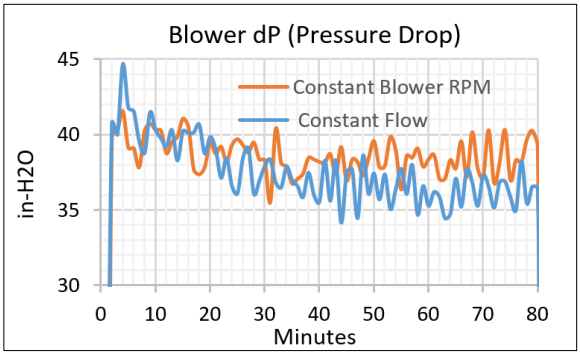

Figure 7. Blower dP at constant RPM and Flow

We designed a bed re-pressurization element into the new MSFC designed dust-tolerance valve. At the half cycle change, the adsorbent bed is under vacuum conditions and re-pressurizes to near-ambient conditions when the selector valve changes as shown in figure 8. The re-pressurization feature softeners the in-rush of air into the adsorbent bed, limiting motion of the adsorbent material because air velocity is reduced.

Inlet air temperature and dew point affect the air temperature exiting the desiccant bed. Increasing air temperature decreases the H2O adsorption capability of desiccant bed Silica Gel. Increasing inlet air dew point increases the mass of adsorbed water, which released more heat-of-adsorption and increases the desiccant bed outlet temperature, shown in figure 9. Long duration testing will be required to determine if warmer (cabin air) conditions would eventually cause H2O breakthrough in the desiccant bed.

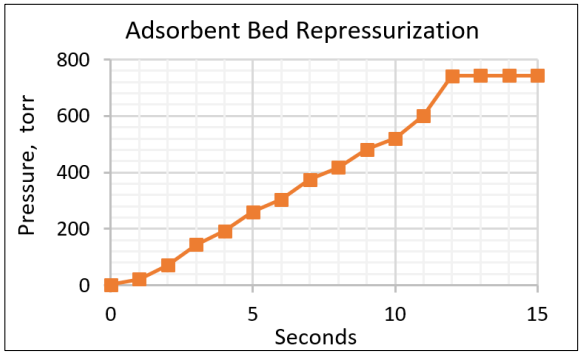

Figure 8. Adsorbent Bed Re-pressurization

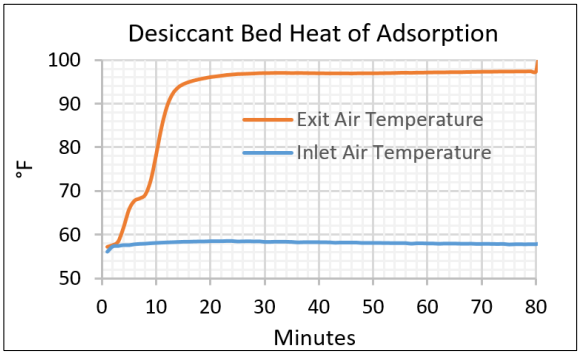

Figure 9. H2O Heat of Adsorption Effect on Air

V. Performance Metrics

A. Drying Over Time

Heritage systems used ASRT (5A) in the adsorbent bed, and 400F bake-out conditions were adequate to remove all moisture prior to system testing. Because ASRT (5A) is no longer available, 4BCO2 uses Grace 544 13X for higher CO2 adsorption. However, Grace 422 13X requires an excess of 400F to remove all moisture. Because bed seals are limited to 400F, we cannot completely remove all moisture from the adsorbent bed 13X prior to system integration. Even small amounts of H2O in the adsorbent bed has a large effect on CO2 removal. The residual moisture is removed during normal system operation even at 400F due to the high performance of the desiccant beds.

Table 2

Inlet air flow	Inlet Air Temp	Inlet air Dwp	ppCO2	hc	PC H2O temp	PC H2O Flow
26 scfm	56 F	49 F	2 torr	10-60-10	51 F	0.52 gpm

Conditions controlled constant for drying test series

CO2 removal increases dramatically over the first 2 weeks of continuous operation as shown in figure 10. CO2 removal performance continues to increase after 30 days of testing, but at a reduced rate shown in figure 11.

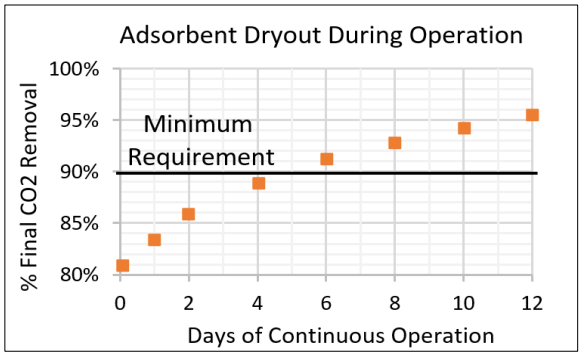

Figure 10: Early System Drying

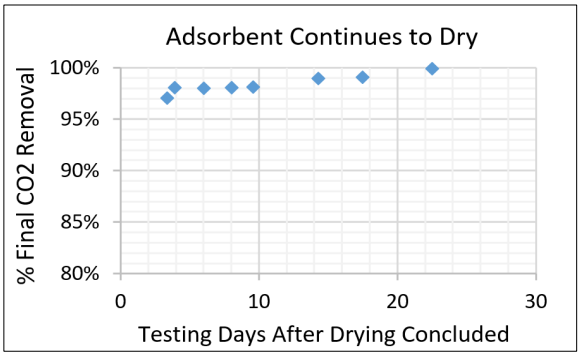

Figure 11: System Dries During Test Program

As run time accumulates, System CO2 breakthrough occurs later, as shown in figure 12. Drying neared completion after 17.5 days as indicated by the similarity of the last two breakthrough traces. The reduction of CO2 removal due to system hold-up also declines as run duration accumulates shown in figure 11.

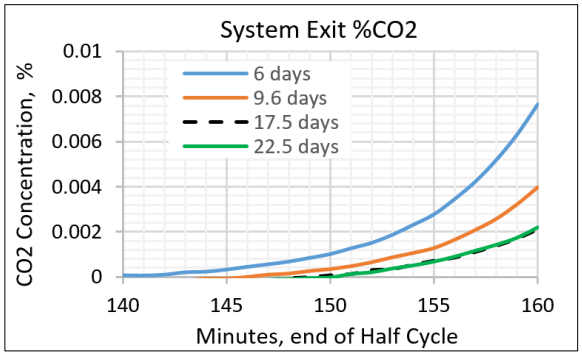

Figure 12: System CO2 Breakthrough Over Time

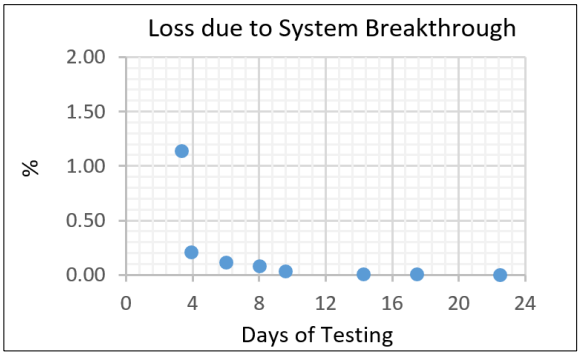

Figure 13: Diminishing loss over time

B. CO2 Removal and System dP (Delta Pressure) vs Air Fow Rate

The system air flow rate is related to the capacity of the blower and the flow resistance of the system. In a prior test series, the Honeywell blower operating at a maximum RPM of 150,000, created an airflow of 27.5 SCFM with an associated half-cycle-dP average of 39.5 in-H2O. The flight system dP will differ due to altered duct geometry. Reducing system volume to fit in the ISS requirement created more duct bends, which drove the decision to use less-flow-resistance additive manufacturing designs to recover pressure loss.

Table 3

Inlet air flow	Inlet Air Temp	Inlet air Dwp	ppCO2	hc	PC H2O temp	PC H2O Flow
21-28 scfm	56 F	49 F	2 torr	10-60-10	51.5 F	0.52 gpm

Conditions controlled constant for air flow test series

We targeted 26 scfm flow because we can operate the Honeywell blower lower than its maximum RPM, while providing surplus CO2 removal performance to compensate for the inevitable losses that occur when implementing systems in operational environments. The efficiency peaks near 26 scfm air flow, as shown in figure 14. These graphs were created holding ppCO2 = 2 torr constant using half cycle duration of 80 minutes. The efficiency peak and total removal rate will change if inlet ppCO2 increases to 3 torr.

The average heater power varied by 20 watts over the flow range. The bed heaters stayed on longer when the air flow was higher, as shown in figure 15. This could be attributed to increased heat loss from the adsorbent bed due to a higher convective environment on the desiccant bed side of the check valve. The beds are isolated with standoffs and thermal insulation. CDRA-4EU required 810 watts average power for a comparable 80 minute half cycle

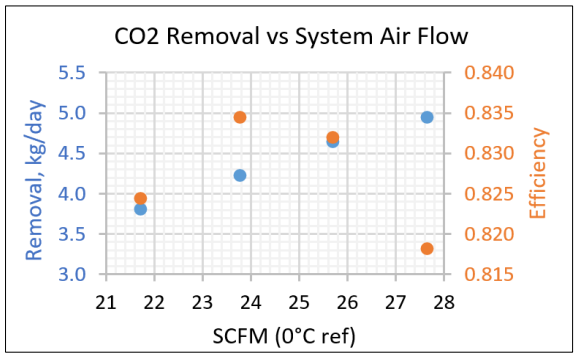

Figure 14: CO2 Removal and Efficiency vs Air Flow

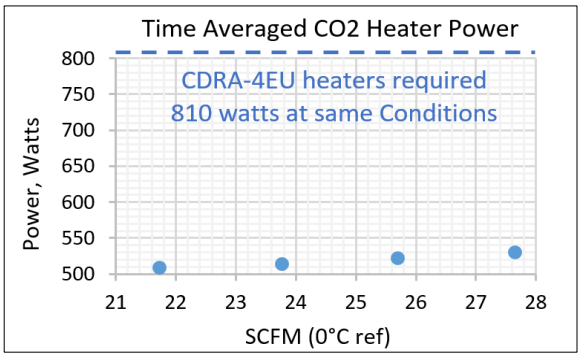

Figure 15: Heater Power vs Air Flow

Precooler exit air temperature increases as the mass of air increases as shown in figure 16. The efficiency of the precooler is high enough to remove most of the additional heat. Adding 27% more thermal air mass increased the air temperature rise across the precooler by only 2.5F (5%).

Figure 17 directly plots the CO2 removal rate as a function of system dP for this specific test series. It is intended to approximate the effect of adding flow resistance if the blower capacity was fixed. For example, if the blower is fixed at a half-cycle-average of 37 in-H2O (max rpm) and we add 5 in-H2O of pressure drop due to ducting, we reduce CO2 laden air-flow which in turn reduces the removal rate by 0.4 kg/day.

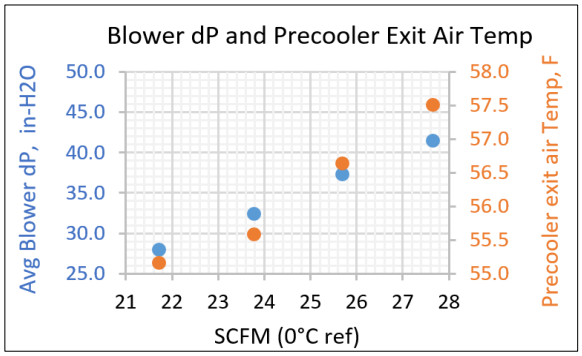

Figure 1: Blower dP and PC Exit Temperature

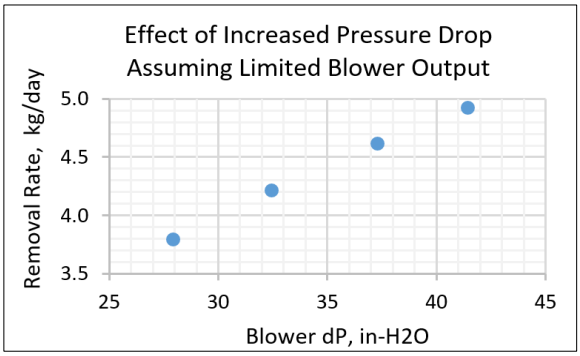

Figure 17: Plotting dP vs Removal Rate for this Series

C. CO2 Removal Rate vs ppCO2

Table 4

Inlet air flow	Inlet Air Temp	Inlet air Dwp	ppCO2	hc	PC H2O temp	PC H2O Flow
21-28 scfm	56 F	49 F	**2-4 torr**	10-60-10	41 F	0.52 gpm

Conditions controlled while varying the ppCO2 at the air system inlet

Half cycle duration was held constant for this test series. The 80 minute half cycle is close to optimum for an inlet ppCO2 concentration = 2 torr. However, we could increase CO2 removal if air inlet ppCO2 = 3 torr by reducing the half cycle time, which would diminish system CO2 breakthrough.

CO2 removal rate increases, Figure 18, with increasing ppCO2 due to the increasing adsorbent capacity at higher CO2 concentrations. This test removed more than 6 crew CO2 levels when operating at an inlet ppCO2 = 3 torr. CO2 removal can be increased further with bed heater and half cycle timing optimization.

Loss due to hold-up only increases slightly, as shown in the initial spike in figure 19. Increasing inlet ppCO2 from 2 torr to 3 torr causes a faster system CO2 breakthrough, but the increased loss is smaller than the amount of CO2 added at the system inlet by a ratio of 8:1.

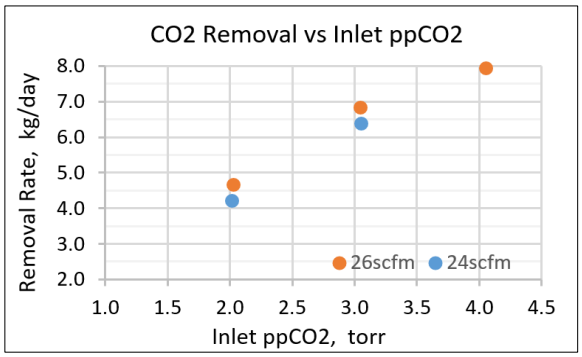

Figure 18: Removal Rate vs ppCO2

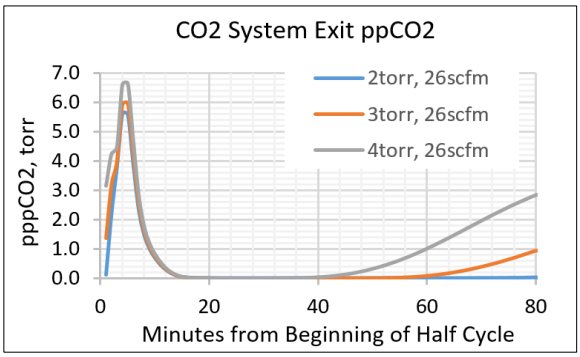

Figure 19: System CO2 Breakthrough vs ppCO2

D. CO2 removal vs LTL Parameters

Table 5

Inlet air flow	Inlet Air Temp	Inlet air Dwp	ppCO2	hc	PC H2O temp	PC H2O Flow
26 scfm	56 F	49 F	2 torr	10-60-10	41-51F	.12-.52 g/min

Conditions controlled while varying the ppCO2 at the air system inlet

13X adsorption capacity diminishes as temperature increases. The precooler removes heat added by the blower and desiccant bed H2O heat-of-adsorption. The heritage CDRA system was designed for an LTL water temperature of 40F, and a maximum flow rate of 0.52 gpm (262 lb/hr). The LTL temperature for the 4BCO2 flight experiment is expected to be 49F at the time of writing. The flight version of new precooler manufacture by the Mezzo corporation will be less efficient than the Linus version because heater transfer surface area was reduced to add redundant seals.

The Mezzo precooler performed exceptionally well, with the outlet air temperature only 6.5F higher than the water inlet temperature at .42 gpm (~200 lb/hr), shown in figure 20.

System CO2 removal performance drops dramatically when the precooler outlet air temperature exceeds 60F, shown in figure 21. A robust system design solution would produce a precooler outlet air temperature near 56F to account for variations in water flow and temperature that occurs when sharing resources onboard ISS.

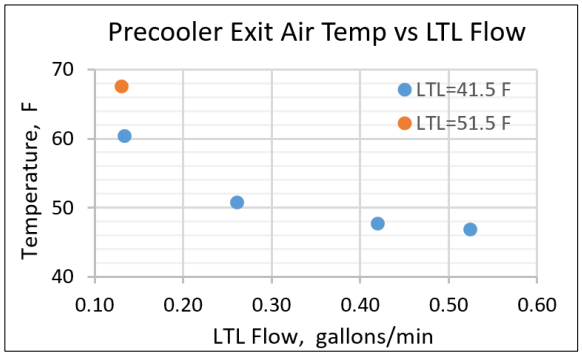

Figure 20: Precooler Exit Air Temperature Variation

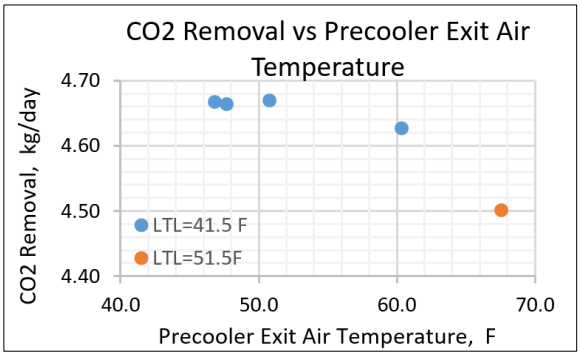

Figure 21: CO2 Removal vs Precooler Air Temperature

The precooler outlet air temperature has a minor effect on the average half cycle heater power, shown in figure 22. If a bed starts the adsorption cycle at a colder temperature, more power and time is necessary to heat the bed to 400F.

The previous figures were created from data averaged over 4 complete cycles, each at a constant set point. Data shown in figure 20 was collected in one minute intervals during the last 20 minutes of a single half cycle when the system thermal behavior is nearly constant. This allowed us to collect 12 test points in 20 minutes instead of 6 continuous days of operation. From Figure 23 and Figure 18, the maximum flow of 262 lb/hr is the maximum amount available on ISS. An LTL flowrate of ~200 lb/hr provides some relief to the ISS team managing resources, while maintaining distance from a condition that could substantially reduce CO2 removal performance.

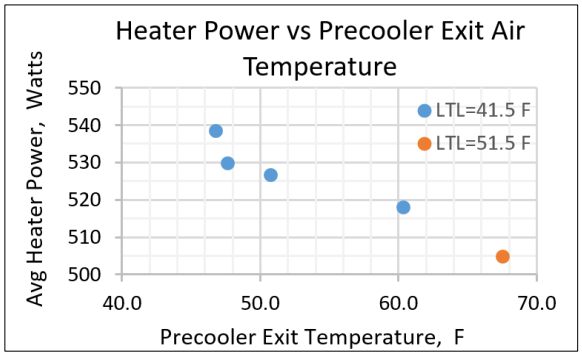

Figure 22: Heater Power vs Precooler Exit Temperature

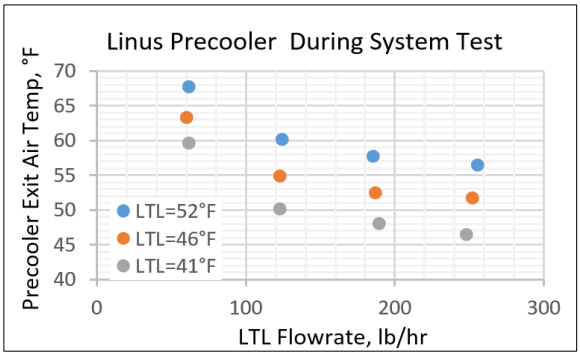

Figure 23: 1 minute variations during a single half-cycle

E. CO2 removal vs Air-Save Segment Elapsed Time

Table 6

Inlet air flow	Inlet Air Temp	Inlet air Dwp	ppCO2	hc	PC H2O temp	PC H2O Flow
26 scfm	56 F	49 F	2 torr	Varied	41 F	0.52 gpm

Conditions controlled while varying the air-save segment timing (nominal is 10 minutes)

The resistance of the rebuilt heater core used in Linus was higher than expected, delivering a power of 700 watts, 50 watts lower than the previous 4BMS-X heater configuration. A power of 700 watts heats the bed to 400F in ~62 minutes, which is faster than required for even the shortest likely (80 minute) half cycle.

Based on the previous test series, we hypothesize higher power early in the cycle drove CO2 out of the 13X when the CO2 flow peaked at ~25 minutes into the half cycle. To test this effect on Linus with minimal software changes, we decreased the air-save segment time, which in turn powered up the secondary heaters earlier. The team also desired to reduce air-save pump run time to extend pump life. Reducing the air-save segment duration will affect the amount of air lost to vacuum and change air purity, but we will quantify that effect in later testing. The primary purpose of this test was to determine if additional heat earlier in the half cycle would increase CO2 Removal.

Shorter air-save duration powers secondary heaters earlier, figure 24. Secondary heaters deliver 71% of the total power[7]. Adsorbent Bed temperature rises faster with a shorter half cycle, figure 25. Bed temperature is 11F higher at 25 minutes, when the peak CO2 adsorption occurs. See Figure 28 and Figure 29. The CO2 removal increased by 2% when the air-save time was reduced from 10 minutes to 6 minutes, the shortest likely air-save time shown in figure 29. This effect is fairly small when the system is operated at an inlet ppCO2 of 2 torr, but we anticipate the effect will be more pronounced at 3 torr when CO2 loading levels are higher. The half cycle average heater power only increases 7 watts when reducing the half cycle from 10 to 6 minutes, shown in figure 27.

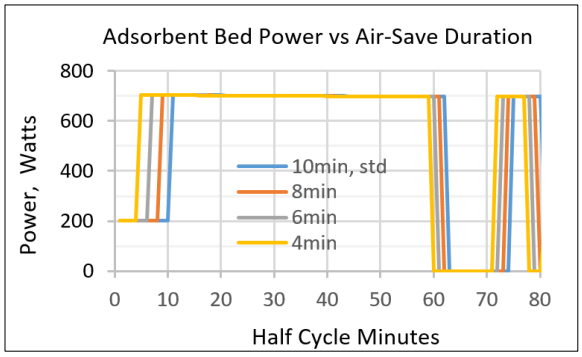

Figure 24: Heater Timing based on Air-Save Time

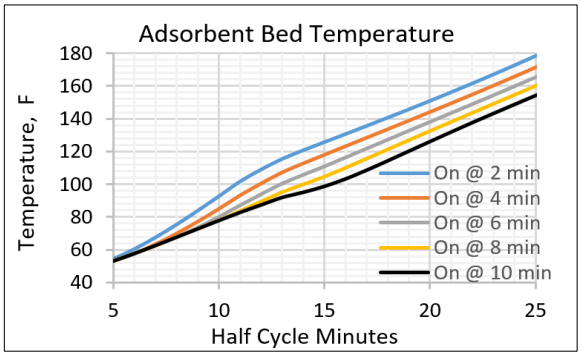

Figure 25: Adsorbent Bed Temperature Response

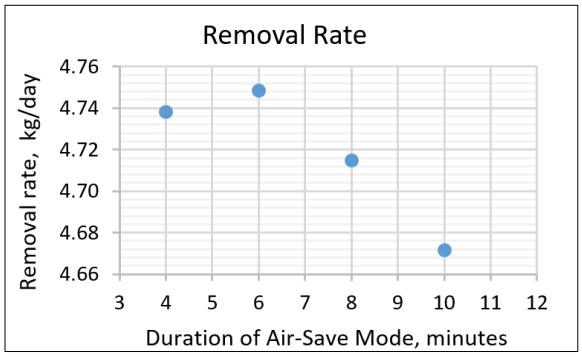

Figure 26: CO2 Removal Rate vs Air-Save Duration

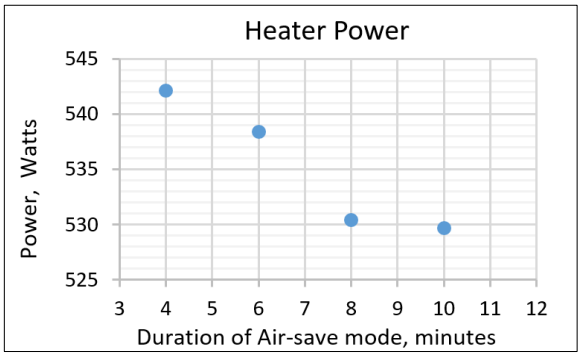

Figure 27: Average Power Increase with Shorter Air Save

The CO2 exit pressure is measured between valve 105 and valve 106, figure 25. The CO2 exit pressure peaks ~25 minutes into the adsorption cycle and coincides with the maximum flow of CO2 to the CO2 exit. The maximum pressure from the time trace in Figure 28 was extracted and placed on figure 29.

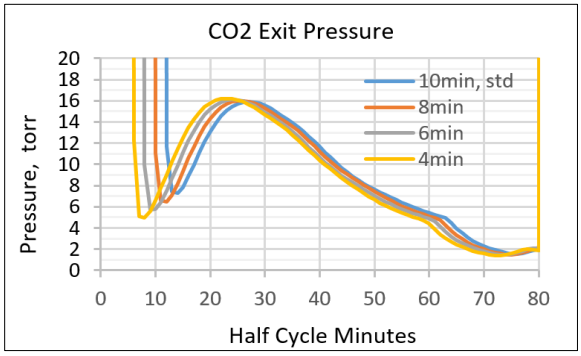

Figure 28: CO2 Exit Pressure vs Time

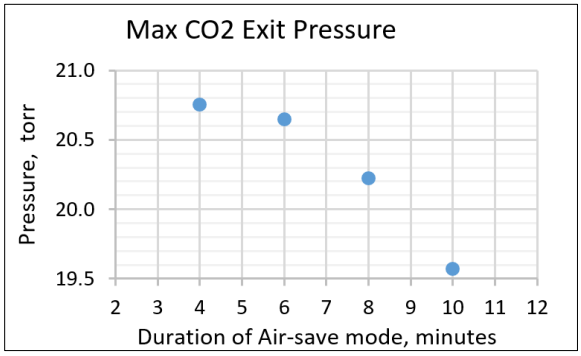

Figure 29: Peak CO2 Pressure from Figure 2

F. CO2 removal vs Secondary Heater Activation Time

Table 7

Inlet air flow	Inlet Air Temp	Inlet air Dwp	ppCO2	hc	PC H2O temp	PC H2O Flow
26 scfm	56 F	49 F	2 torr	10-60-10	41 F	0.52 gpm

Conditions controlled while varying the initiation time of the secondary heaters

After the previous air-save duration test series, we modified the control software to allow independent control of the secondary heater timing and air-save segment duration. For this test series, the air-save segment was held constant at 10 minutes and the secondary heaters were initiated earlier in 2 minute increments. Each test operated for more than 4 complete cycles

Independently decreasing the secondary heater timing, shown in figure 30, created the same adsorbent bed temperature response as when we reduced the air-save segment timing: 11F at 25 minutes into the half cycle with a 4 minute time advance.

Advancing the time of secondary heater activation produced a similar increase in CO2 removal similar as reducing air-save segment duration, shown in figure 31. In the next Linus test series, we will test the conditions where we activate the secondary heaters for the full duration of the half cycle while decreasing the air-save time to ~ 6 minutes.

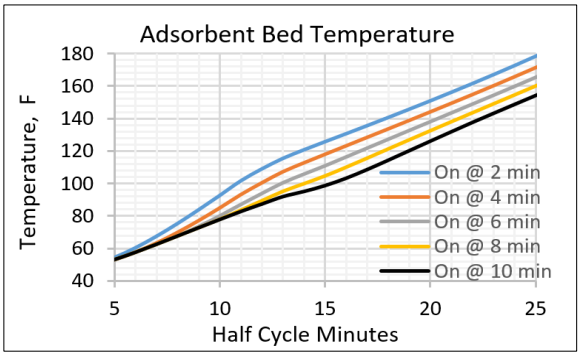

Figure 30: Bed Response with Early Secondary Heaters

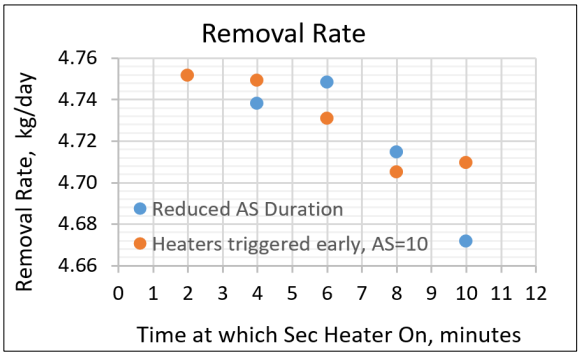

Figure 31: Removal Rate vs Secondary Heater Timing

CO2 removal vs Inlet Air Temperature and Dew Point

Table 8

Inlet air flow	Inlet Air Temp	Inlet air Dwp	ppCO2	hc	PC H2O temp	PC H2O Flow
26 scfm	55-75F	Variable, 1 test	2 torr	10-60-10	41 F	0.52 gpm

Conditions controlled while varying air inlet temperature

CO2 removal increases with inlet air temperature, figure 32 CO2 removal increases because the decrease in holdup loss (2%) exceeds the increase in breakthrough loss (.08%), shown in figure 33. Higher air temperature warms the silica gel, diminishing silica H2O adsorption, shown in figure 34. More H2O is pushed to the desiccant bed 13X, which pushes the adsorbed CO2 to the adsorbent bed. CO2 removal increases because more CO2 is entering the adsorbent bed. Note decrease in the air exit CO2 levels at the beginning of the half cycle, figure 34.

Due to high precooler efficiency, shown in figure 35, an 18F increase in inlet air temperature is converted to only 0.6 F increase in adsorbent bed temperature, diminishing the effect of higher temperature in the adsorbent bed.

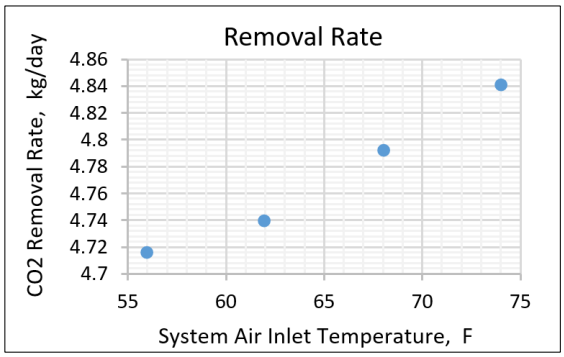

Figure 32: CO2 Removal vs Inlet Air Temperature

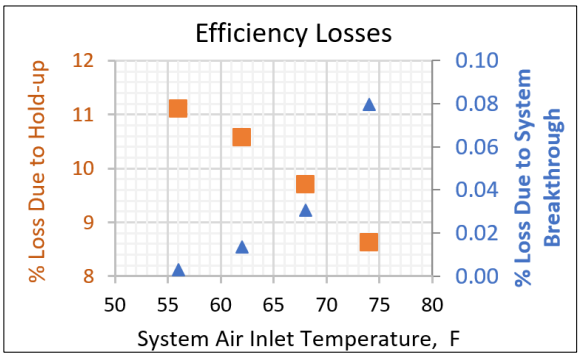

Figure 33: Source of CO2 Removal Improvement

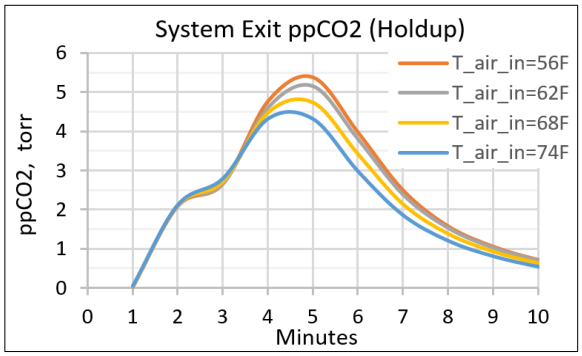

Figure 34: Change in CO2 Holdup

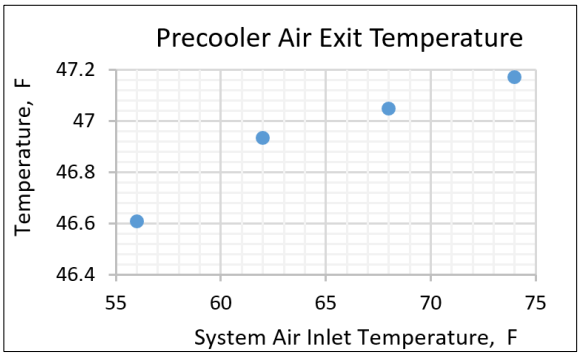

Figure 35: Change in Precooler Exit Air Temperature

Increasing the inlet air temperature increases the air temperature conducted through valve 101, valve 102 and valve 103, shown in figure 36. The valve seal material limit is 400F. Both the valve body and drum are made from aluminum and the difference in thermal growth should be minimal as temperature increases. However, the valves will be tested to a value between 100F and 150F for other reasons, and the valves will likely be assigned that value as the *maximum operational temperature*.

We ran a single case at very low inlet air dew point to remove residual moisture from the system from the elevated air temperature tests, shown in figure 37. The system exit air temperature increased significantly because the low dew point contributes less H2O mass into the desiccant beds. At the half cycle change, less H2O mass takes up less heat, so more of the heat energy from the adsorbent bed is translated into higher air temperature. This low dew point will not occur on ISS, but was considered for ground test phases where high purity air was a convenient choice.

Warmer air temperature improves aspects of performance shown in figure 37, but the possibility exists that this could cause H2O breakthrough in the desiccant bed in the long term. This characteristic will be tested in the future.

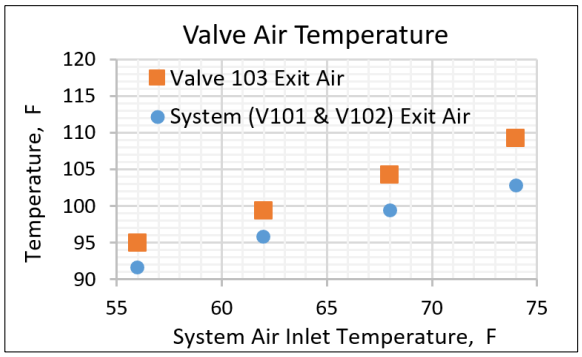

Figure 36: Maximum Valve Temperature

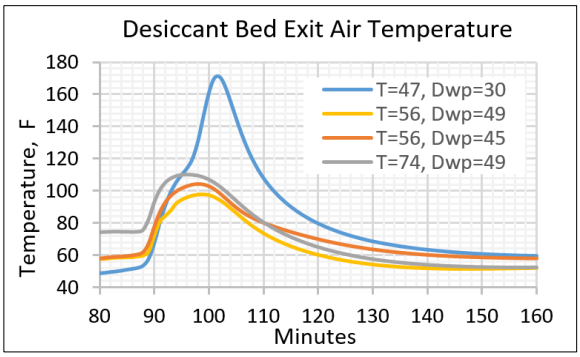

Figure 37: Effect of Low Dew Point and Temperature

VI. Conclusions and Recommendations

We have concluded the initial test phase that individually quantified the system responses to various boundary conditions and system test parameters. The 4BCO2 bed volume and mass is >20% less than CDRA, while maintaining a CO2 removal performance significantly higher than the 4.16 kg/day requirement with inlet air CO2 partial pressure of 2 torr. The 4BCO2 average heater power usage is only 63% of CDRA. A flight blower controller and a more-flight-like Celeroton blower will be installed in the next hardware configuration. We will then optimize the cycle for exploration requirements and ISS environments.

Acknowledgments

The authors of this work would like to acknowledge the contributions of the ES62 technicians, mechanical designers, machinists, controls engineers, and the MSFC propulsion team who delivered the new valve design.

References

1. Peters, W.P.;Knox, J.C., *4BMS-X Design and Test Activation*, 47th ICES Conference, 2017.
2. Cmarik, G. E.; Knox, J. C.; Peters, W.P., *4-Bed CO2 Scrubber – From Design to Build*, 50th ICES conference, 2020.
3. Cmarik, G. E.; Knox, J. C., *CO2 Removal for the International Space Station–4-Bed Molecular Sieve Material Selection and System Design*. 2019.
4. Knox, J. C.; Gauto, H.; Miller, L. A. *In Development of a Test for Evaluation of the Hydrothermal Stability of Sorbents used in Closed-Loop CO2 Removal Systems*, International Conference on Environmental Systems, Bellevue, Washington, Bellevue, Washington, 2015.
5. Knox, J. C.; Cmarik, G. E.; Watson, D. W.; Giesy, T. J.; Miller, L. A., *Investigation of Desiccants and CO2 Sorbents for Exploration Systems 2016-2017*. In 47th International Conference on Environmental Systems, Charleston, 2017.
6. Cmarik, G., Knox, J., & Huff, T. (2018, July). Analysis of Performance Degradation of Silica Gels after Extended Use Onboard the ISS. 48th International Conference on Environmental Systems.
7. Schunk, R.G.; Peters, W.T.; Thomas, J.T., *Four Bed Molecular Sieve - Exploration (4BMS-X) Virtual Heater Design and Optimization*, ICES conference, 2017